

Article ID: 1007-8827(2011)06-0470-09

The role of surface oxygen-containing functional groups in liquid-phase adsorptive denitrogenation by activated carbon

LI Na^{1,2}, Masoud Almarri², MA Xiao-liang², ZHA Qing-fang¹

(1. College of Chemistry and Chemical Engineering, China University of Petroleum, Dongying 257061, China;

2. EMS Energy Institute, The Pennsylvania State University 209 Academic Project Building, University Park, PA 16802, USA)

Abstract: Twelve activated carbon (AC) samples with different physical and chemical properties were selected to investigate their ability for the adsorptive denitrogenation of liquid hydrocarbons using two model fuels containing typical nitrogen compounds, indole and quinoline in decane. The surface oxygen-containing groups of the ACs were characterized by temperature-programmed desorption with a mass spectrometer to identify and quantify the type and concentration of the oxygen-containing functional groups based on the CO- and CO₂-evolution profiles. The adsorption behavior of AC for nitrogen compounds in decane was found to obey the Langmuir adsorption isotherm. The adsorption parameters (the maximum capacity and the adsorption constant) were estimated. With these results, the correlation between the adsorption performance of the AC samples and their physical/chemical properties was evaluated by a multiple linear-regression analysis, which indicated that the physical properties were not the key factors for the removal of the nitrogen compounds in decane. Furthermore, the oxygen-containing groups of ACs, especially the carboxylic acid groups, were found to be mainly responsible for nitrogen adsorption.

Keywords: Activated carbon; Surface oxygen-containing groups; Adsorptive denitrogenation; Multiple linear regression analysis

CLC number: TQ 424.1

Document code: A

1 Introduction

Deep denitrogenation of liquid hydrocarbon streams has attracted great attention from the refinery industry, because the nitrogen compounds coexisting in the liquid-hydrocarbon streams strongly inhibit ultra-deep hydrodesulfurization (HDS) and further poison many catalysts that are used in subsequent processes, including hydrodearomatization, hydrocracking, and reforming^[1-7]. In addition, denitrogenation is one of the major tasks in the upgradation of coal-derived liquids and other liquid hydrocarbons used for the production of clean transportation fuels^[8-13]. Currently, removal of nitrogen from various liquid hydrocarbon streams is mainly carried out by the catalytic hydrodenitrogenation (HDN) process in refineries^[9-10,14-16]. However, HDN is more difficult to conduct than HDS, because severe reaction conditions and a high hydrogen consumption are required^[17-18]. Therefore, adsorptive denitrogenation (ADN) of liquid-hydrocarbon streams using adsorbents with high selectivity

has attracted great attention^[8,12,19-21]. Some investigations on the ADN of liquid hydrocarbons on activated carbons (ACs) have been reported recently in literature^[8,11,12,19]. ACs, due to their high adsorption capacity, selectivity, and good regenerability, have been found to be very promising adsorbents for the selective removal of nitrogen compounds^[8,19].

In general, the adsorption behavior of carbon materials depends on both the physical and the chemical properties of the materials. However, previous studies have indicated that, in the liquid phase, the surface chemical structure of ACs plays a dominant role in determining the adsorption performance, regardless of the physical structure that comprises the total surface area and the micro- and mesoporous structure^[22]. The adsorption capacity for nitrogen compounds increases with the total oxygen concentration on the surface of AC, whereas micropore volume does not show any obvious effect on the adsorption performance^[22]. Further investigations showed that

Received date: 2011-05-05; **Revised date:** 2011-12-30

Corresponding author: ZHA Qing-fang, Professor. E-mail: chaqingf50@hotmail.com

Author introduction: LI Na (1982-), female, Ph. D. Student, engaged in research of the adsorptive denitrogenation of liquid hydrocarbon streams. E-mail: leenaa82@hotmail.com

English edition available online ScienceDirect (<http://www.sciencedirect.com/science/journal/18725805>).

DOI: 10.1016/S1872-5805(11)60093-0

the oxygen-containing functional groups on the AC surface play a dominant role in the ADN on AC^[22]. The widely accepted predominant functional groups present on the surface of ACs are the carboxyl, anhydride, lactone, phenol, carbonyl, and quinone groups^[22-23]. Among them, the carboxyl, anhydride, lactone, and phenol groups are considered the acidic type group, whereas the carbonyl and quinone groups are the basic groups. The acidic groups contribute more toward adsorption of the basic nitrogen compounds, whereas the basic oxygen-containing groups may contribute more to the adsorption of neutral nitrogen compounds. Thus, the ADN performance of the carbon-based adsorbents can be improved significantly by enhancement of the desired oxygen-containing functional groups on the surface.

In spite of many studies on the ADN of liquid-hydrocarbon streams over ACs, the mechanism of ADN on ACs, especially, the influence of the surface chemistry of AC, has not been well clarified^[8,19,22]. To develop high-performance carbon-based adsorbents for the ADN of liquid-hydrocarbon streams, understanding (1) the fundamental role of the type and concentration of the carbon-surface oxygen-containing functional groups present on the carbon surface and (2) their effect on the performance of ADN is crucial.

The present study focuses on examining the effect of the surface chemistry, the type and amount of the oxygen-containing functional groups on the adsorption performance. It was reported that Quinoline and indole have been reported to be the main nitrogen compounds in different liquid-hydrocarbon streams^[24-26]. Here, the adsorption performance of twelve representative carbon-based adsorbents for these two typical nitrogen compounds, quinoline (basic) and indole (neutral), was evaluated in a batch-adsorption system using two model solutions. To build a structure-performance relationship for the ADN on ACs, the type and the concentration of the oxygen-containing functional groups on the carbon surface were characterized by the temperature-programmed desorption method (TPD), which was modified based on previous procedures^[22,27-28]. A vast amount of work has shown that the TPD method is especially adequate for the identification and quantification of the oxygen-containing functional groups on carbon materials^[23, 29-33]. The measured types and concentrations of the various oxygen-containing functional groups on the AC samples were correlated with their ADN performance. The contribution of each oxygen-containing functional group on the carbon surface to the adsorption of both basic and neutral nitro-

gen compounds was estimated by multiple linear-regression analysis. The regression coefficient showed the relative contributions of the different types of oxygen-containing functional groups on the adsorption of nitrogen compounds.

2 Experimental

2.1 Carbon materials

Twelve AC samples with different physical and chemical properties were used in this study. Table 1 shows the sources and BET surface areas of these AC samples, which are denoted as AC1, AC2, AC3, AC4, AC5, AC6, AC7, AC8, AC9, AC10, AC11, and AC12. Before using them in the experiments, all the samples were pretreated at 110 °C in a vacuum oven overnight for removal of moisture and other adsorbed volatile contaminants. Quinoline (with a purity of 98%), indole (with a purity of 99%), and decane (with a purity of 99%) were purchased from Sigma-Aldrich Chemical Co. and used without further purification.

Table 1 Source and BET surface area of the tested AC samples

Sample ID	Source	Maker	$S_{\text{BET}}/\text{m}^2 \cdot \text{g}^{-1}$
AC1	pet. coke	HORI *	1080
AC2	pet. coke	HORI	851
AC3	pet. coke	HORI	1357
AC4	pet. coke	HORI	1100
AC5	pet. coke	HORI	1036
AC6	coal	EMS Energy Institute	1050
AC7	coconut	Calgon	993
AC8	wood	WESTVACO	1603
AC9	wood	WESTVACO	2320
AC10	pet. coke	Kansai	2263
AC11	lignite coal	Norit	650
AC12	coal	Norit	1151
OAC10 [#]	pet. coke	EMS Energy Institute	1438

* HORI: Heavy Oil Research Institute, China University of Petroleum

[#]This sample was an oxidized sample of AC10 by $(\text{NH}_4)_2\text{S}_2\text{O}_8$ (APS) at 60 °C, for 3 h with 2.0 mol/L APS solution in 1 mol/L H_2SO_4 , which was prepared in EMS Energy institute.

2.2 Characterization of AC samples

2.2.1 Textural structure

The textural characterization of the materials was carried out by studying the adsorption/desorption of nitrogen at 77 K using an ASAP2010 surface area and porosimetry analyzer. Standard Brunauer, Emmett and Teller (BET) and Dubinin and Radushkevich (DR) models were applied, respectively, to derive the surface area and the micropore volume. The pore-size distribution was calculated according to the density functional theory (DFT) method.

2.2.2 TPD-mass spectrometry

The oxygen-containing functional groups on the carbon surface were analyzed and quantified by TPD using the AutoChem2910 (Micromeritics Instrument Co., Georgia, USA) with a mass spectrometer. Helium gas, charged with 5% argon as the internal standard, was used as the carrier gas for TPD characterization. Approximately 100 mg of the sample were placed in a quartz reactor. The reactor was then connected to the instrument. After drying the sample at 110 °C for 2 h under helium flow at 50 mL/min, the temperature was increased to 1050 °C at a rate of 10 °C/min under helium flow at 50 mL/min (under standard temperature and pressure). The CO, CO₂, and H₂O evolved were continuously measured using a quadruple mass spectrometer (Dycor, Model 2000). The evolved gases were quantified by integration of the peak area and the subsequent calibration with calcium oxalate standard. All the integrated peak areas were calibrated using the value of the argon signal (internal standard) to correct the error caused from equipment and other influences. The detailed information about both the type and the concentration distribution of the surface oxygen-containing complexes was obtained by the modified deconvolution procedure of the TPD-MS spectra based on the method previously described by Figueiredo and coworkers^[22, 27-28].

2.2.3 Diffuse-reflectance infrared spectroscopy

The spectra from diffuse-reflectance infrared spectroscopy (DRIFTS) were collected using a FTIR-3000 spectrophotometer equipped with a diffuse-reflectance attachment. The carbon materials were dried at 110 °C under vacuum before IR evaluation. The samples were finely ground to a powder in an agate mortar and then mixed with KBr at a mass ratio of 1 : 60. The background was measured based on KBr. Four hundred scans were taken at a resolution of 2 cm⁻¹.

2.3 Adsorption experiments and analysis of treated oil samples

Two solutions, S-1 and S-2, containing 20.0 μmol/g of quinoline and indole in decane, respectively, were prepared for use in evaluation of the adsorption behavior of the AC samples toward acidic and neutral nitrogen compounds. The adsorption tests with different solution/adsorbent weight ratio were conducted in a batch-adsorption system with magnetic stirring at 300 r/min at room temperature for 4 h. After the desired adsorption time, the mixture was filtered. The total nitrogen concentration in the treated solution was analyzed using an ANTEK 9000 series nitrogen analyzer.

3 Results and discussion

3.1 Characterization of the surface chemistry of ACs

To clarify the relationships between the adsorption behaviors of different oxygen-containing groups and different types (basic or neutral) of nitrogen compounds, twelve active carbons with different concentrations and distributions of the surface oxygen-containing groups were selected as the adsorbents for ADN investigation. The BET surface areas of these ACs are summarized in Table 1, which range from 650-2 263 m²/g, with the largest difference being ~3.5 times. The oxygen-containing functional groups were characterized by DRIFTS. The spectra of two typical samples (unoxidized and oxidized samples, AC10 and OAC10, respectively) are shown in Fig. 1. Three main bands can be identified in the spectra, which confirmed the existence of oxygen-containing functional groups. The first one at 1735 cm⁻¹ was associated with C=O in lactones, carboxylic acids, and anhydrides; the second one was close to 1 600 cm⁻¹, related to quinone and similar groups; and the broad one centered at 1 235 cm⁻¹ was characteristics of C—O stretching in ethers, lactones, phenols, and carboxylic anhydrides. The intensity of these three peaks was stronger in OAC10 than those in AC10, which indicated that the amount of oxygen-containing groups was increased after oxidation. However, determining the amounts of the different groups through DRIFTS was very difficult due to the overlap in the peaks of similar groups. To obtain qualitative and quantitative information on the individual functional groups of the carbon materials, TPD was used in this work. The CO- and CO₂-evolution profiles were recorded with a mass spectrometer. This technique is based on the observation that essentially all the reactive organic oxygen-containing functionalities decompose to form CO and CO₂ at different ranges of temperatures during a temperature-programmed heat treatment of ACs reaching up to 1050 °C under an inert atmosphere^[16, 19-20].

The typical CO and CO₂ profiles of ACs are presented in Fig. 2. The obtained CO- and CO₂-evolution profiles were further deconvoluted by the method reported by Figueiredo and coworkers^[27-28]. The deconvoluted peaks can be assigned as follows: For the CO₂-evolution profiles, the peaks around 280 and 400 °C were assigned to the carboxylic groups of strong and weak acids, respectively. The anhydride groups decompose at 540 °C. The peaks at 650 and 800 °C can be assigned to the decomposition of lactones with different chemical environments. For the

CO-evolution profiles, the peaks at 300 and 420 °C were assigned to the decomposition of strong and weak acid groups, respectively. The peaks at 550, 680, 800, and 1 020 °C were assigned to carboxylic anhydrides, phenols, carbonyl or quinones, and pyrone, respectively. The results showed that the deconvolution procedure fits the data quite well for the CO₂ and CO profiles of all the AC samples. The quantitative analysis of CO and CO₂ was carried out with the standard curve of calcium oxalate after calibrating the signals with argon as the internal standard.

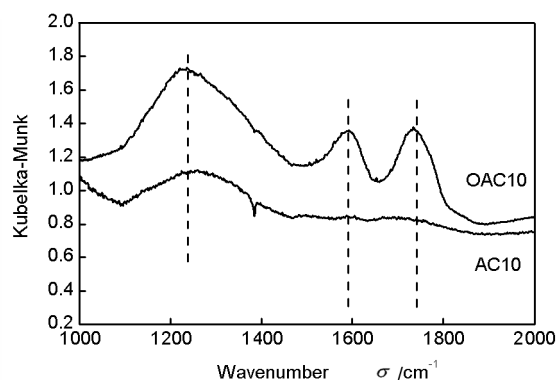


Fig. 1 DRIFT spectra of the sample AC10 and OAC10

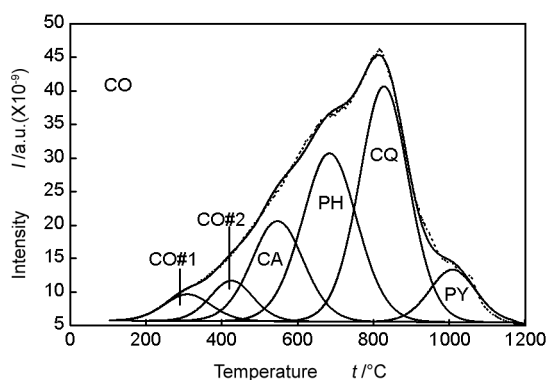
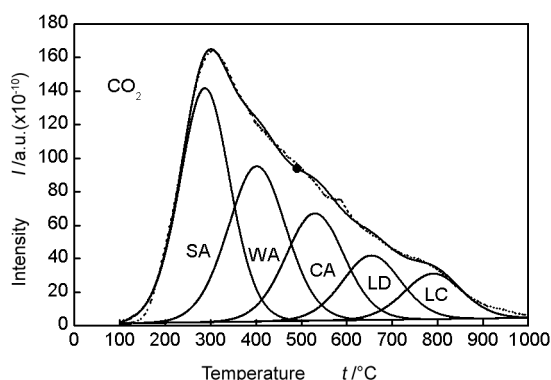


Fig. 2 TPD evolution and deconvolution profiles for released CO and CO₂ of AC7

Table 2 Concentration of various functional groups on the basis of the TPD deconvolution method

Samples	Eq (Qu) ^a / (mg-N)·g ⁻¹	Eq (In) ^b / (mg-N)·g ⁻¹	CA ^c , X1/ μmol·g ⁻¹	An ^d , X2/ mol·g ⁻¹	LA ^e , X3/ μmol·g ⁻¹	PH ^f , X4/ μmol·g ⁻¹	CO ^g , X5/ μmol·g ⁻¹	O ^h / μmol·g ⁻¹
AC1	5.4	5.6	632	306	146	851	998	3719
AC2	4.2	4.2	125	62	57	579	811	2230
AC3	6.3	6.2	1398	639	191	1 065	1019	5201
AC4	4.6	3.9	74	26	62	358	615	1737
AC5	12.8	13.8	1407	600	407	2494	1026	7832
AC6	7.6	12.2	257	107	46	957	940	3726
AC7	5.6	5.5	325	61	104	304	838	2422
AC8	10.7	7.8	303	116	67	1461	937	4207
AC9	8.9	8.3	284	136	128	1993	1064	4837
AC10	11.3	10.6	601	173	82	981	1544	4939
AC11	5.4	4.3	121	87	109	436	896	2345
AC12	2.6	2.1	65	60	96	619	988	2159
OAC10	29.4	28.6	2819	1670	410	3070	3380	16248

a; Equilibrium capacity of quinoline at $5 \cdot 10^{-5}$; b; Equilibrium capacity of indole at $5 \cdot 10^{-5}$; c; Carboxylic acid; d; Anhydride; e; Lactone; f; Phenol; g; Carbonyl/quinone; h; Total oxygen groups.

The amount and distribution of the surface groups on these ACs are summarized in Table 2. These twelve AC samples contained different concentrations of oxygen-containing groups, ranging from 1 737-16248 mmol oxygen per gram AC. The order of the amount of oxygen-containing groups was as follows: AC4 < AC12 < AC2 < AC11 < AC7 < AC1 ~

AC6 < AC8 < AC9 < AC10 < AC3 < AC5 < OAC10. The distribution of the oxygen-containing groups was different for all these ACs. Thus, the wide range of quantities and distributions of oxygen-containing groups on these ACs facilitated the investigation of the relationships between specific oxygen-containing groups and adsorption of nitrogen compounds.

3.2 Adsorption isotherms and parameters of langmuir isotherm

The AC-based adsorbents were mixed with the model fuel by stirring at different weight ratios in the batch-adsorption system at room temperature. The concentrations of the nitrogen compounds in the solution were analyzed at different time intervals. The relationships between the concentration of quinoline and indole and the mixing time (adsorption isotherm) of the 12 AC samples are shown in Figs. 3 and 4 respectively. All the obtained adsorption isotherm curves were of type-I, regardless of the different adsorbents and solutes. For both the nitrogen compounds, the surface areas (micro- and mesoporous surface areas) of the ACs do not have a significant effect on the adsorption properties. The adsorbents based on AC5 and AC12, with similar values of surface area and pore-size distribution, showed significant difference in their adsorption capacities. AC5 with a surface area of 1036 m²/g showed an adsorption capacity of 12 (mg-N)/g and 15 (mg-N)/g for the quinoline and indole solutions, respectively. However, AC12 with a surface area of 1151 m²/g showed an adsorption capacity of only 2.5 (mg-N)/g and 3 (mg-N)/g for the quinoline and indole solutions, respectively. The capacities of the ACs for both these nitrogen compounds have direct relationships with their concentrations of surface oxygen-containing groups. For quinoline, the capacity of the ACs have the order of AC12 < AC4 ~ AC2 ~ AC11 < AC1 ~ AC3 ~ AC7 < AC8 < AC9 < AC10 < AC6 < AC5, whereas, for indole, the following order is found: AC12 < AC2 < AC4 < AC7 ~ AC11 < AC1 < AC3 < AC6 < AC9 < AC8 < AC10 < AC5. The AC samples with more oxygen-containing surface groups have larger absorption capacity. However, the difference in the order of these two different nitrogen compounds indicates different relationships between the nitrogen compounds and the surface oxygen-containing groups.

If the Langmuir adsorption was assumed, the following relationship^[8] should be applied:

$$q = \frac{Kq_m C_e}{1 + KC_e}, \quad (1)$$

where C_e and q are the concentrations of nitrogen in the liquid phase and the adsorbed phase at equilibrium, respectively; K is the adsorption equilibrium constant; and q_m is the maximum adsorption capacity of nitrogen corresponding to the saturation coverage of the surface. Linear regression was conducted between C_e/q and C_e to estimate the values of K and q_m in the Langmuir adsorption equation for each AC sample. The obtained q_m and K values of each AC sample for

indole and quinoline are listed in Table 3. The value of q_m for indole was higher than that for quinoline in all the AC samples, which may be the result of the smaller molecular volume of indole compared to that of quinoline. However, the value of K for quinoline was larger than that for indole, which indicated that the average affinity of the adsorption sites for quinoline was greater than that of the adsorption sites for indole. The equilibrium adsorption capacity for sample AC5 showed the highest value for both quinoline and indole, which correspond to the highest amount of oxygen-containing groups for AC5. However, the adsorption capacity of these two nitrogen compounds show complex relationships with both the total amount of oxygen-containing groups and the distribution of different types of oxygen-containing groups on the surfaces of these AC samples. To obtain further information, the correlation of the different types of oxygen-containing groups with the equilibrium adsorption capacity of quinoline and indole are investigated.

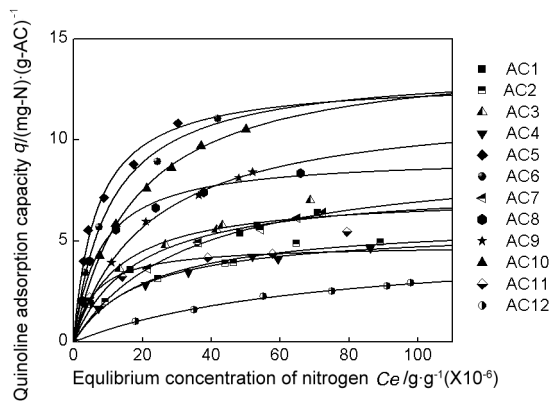


Fig. 3 Adsorption isotherms for quinoline at 25°C on various samples. Symbols represent experimental data, and the lines are based on the estimated Langmuir isotherm equations

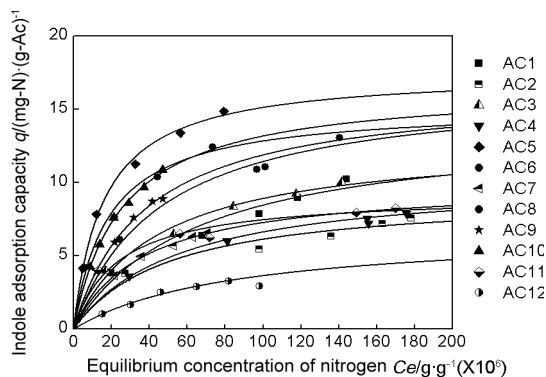


Fig. 4 Adsorption isotherms for indole at 25°C on various samples. Symbols represent experimental data, and the lines are based on the estimated Langmuir isotherm equations

Table 3 Adsorption parameters for idole and quinoline over AC samples on the basis of langmuir adsorption isotherms

Sample	Quinoline			Indole		
	$q_m / (\text{mg-N}) \cdot \text{g}^{-1}$	$K / \text{g} \cdot \mu\text{g}^{-1}$	Equilibrium capacity at $4 \cdot 10^{-5} \text{ g} / (\text{mg-N}) \cdot \text{g}^{-1}$	$q_m / (\text{mg-N}) \cdot \text{g}^{-1}$	$K / \text{g} \cdot \mu\text{g}^{-1}$	Equilibrium capacity at $4 \cdot 10^{-5} \text{ g} / (\text{mg-N}) \cdot \text{g}^{-1}$
AC1	14.0	0.015	5.30	7.7	0.055	5.32
AC2	9.2	0.020	4.08	6.0	0.046	3.90
AC3	12.8	0.023	6.10	7.3	0.081	5.55
AC4	10.3	0.018	4.30	5.6	0.051	3.77
AC5	17.5	0.063	12.52	12.9	0.149	11.08
AC6	16.6	0.022	7.77	13.5	0.095	10.72
AC7	10.0	0.027	5.15	9.2	0.030	5.05
AC8	15.2	0.055	10.40	9.2	0.129	7.70
AC9	16.3	0.027	8.41	11.8	0.046	7.66
AC10	16.5	0.039	10.08	14.3	0.056	9.86
AC11	9.2	0.043	5.81	4.8	0.167	4.18
AC12	6.7	0.012	2.16	5.0	0.014	1.79

3.3 Correlation between nitrogen adsorption capacity and the oxygen-containing functional groups on the surface of the AC samples.

Generally, the adsorption capacity of the AC depends on many factors, including (1) the physical (textural) properties of the AC, such as surface area and pore-size distributions, (2) surface chemical properties, such as type and number of adsorption sites (i. e., surface functional groups), (3) adsorbate and solution characteristics, and (4) adsorption conditions. In this work, we prepared two simple model solutions containing quinoline and indole in decane. This allowed us to directly correlate the adsorption uptake for each molecule with the physical and chemical properties of the AC samples. As reported in our previous work^[22], the surface areas and the pore-size distributions of the studied samples may not play an important role in determination of their adsorption capacities for the nitrogen compounds used in this simple model-fuel adsorption. Therefore, the physical properties were not included in the following correlation between the adsorption capacity and the oxygen-containing functional groups. The results indicate that the types and amounts of oxygen-containing functional groups play a decisive role during the ADN process on the AC adsorbents. A higher concentration of oxygen-containing functional groups results in higher adsorption capacity for the nitrogen compounds. However, the relationships between the different nitrogen compounds and the amounts and distributions of oxygen-containing functional groups on the AC samples are very complex. To analyze this complex relationship, here, the correlation of the adsorption capacity with the amounts of different oxygen-

containing functional groups was analyzed. Assume that the adsorption capacity of the AC samples can be expressed by a linear expression, as shown below:

$$\text{Cap} = \sum_{i=1}^n \alpha_i X_i, \quad (2),$$

where α_i and X_i are the coefficient and the concentration of the oxygen-containing functional group i on the surface. Five different oxygen-containing functional groups, for example, strong and weak carboxylic acid, anhydride, lactone, phenol, and carbonyl, are selected and labeled as X1, X2, X3, X4, and X5, respectively. Based on their F values and R^2 , a linear correlation was observed between the adsorption capacity of the AC samples for different nitrogen compounds and the surface oxygen-containing functional groups. To improve the flexibility of such a model, a special sample denoted as OAC10 (Tables 1 and 2) was included for this multiple linear correlation. The results are summarized in Table 4. For both quinoline and indole, the coefficients of the acidic carboxylic groups are the largest among all the coefficients, for example, 0.68 for quinoline and 0.56 for indole. Such a result indicates that the acidic functional groups appear to be highly responsible for adsorption of the nitrogen compound. In other words, the oxygen-containing functional groups other than acidic groups do not contribute significantly to nitrogen adsorption. This speculation was verified in our laboratory recently by removing the carboxylic groups on the AC surface using heat treatment, which will be published in our next study. The observation that the coefficient of the acidic groups for quinoline is larger than that for indole agreed well with the result of high K value of quinoline compared with that of indole.

Table 4 Correlation of adsorbed quinoline and indole concentration at $C_e = 5 \times 10^{-5}$ associated with various surface functional groups

	Correlation	F^a	R^2
Quinoline	$q_e = 0.68X_1 - 0.14X_2 - 0.84X_3 + 0.07X_4 + 0.06X_5 + 223.6$	2.465E-06	0.98
Indole	$q_e = 0.56X_1 + 0.12X_2 - 1.27X_3 + 0.08X_4 + 0.07X_5 + 317.9$	8.121E-05	0.94

^a F value = $\sum (observed\ value - calculated\ value)$

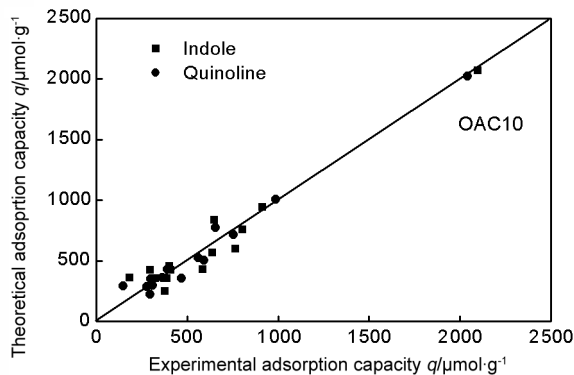


Fig. 5 Correlation between experimentally determined adsorption capacity versus calculated adsorption capacity by linear regression

It should, however, be noted that some of the coefficients in these cases, such as the coefficients of the phenol and carbonyl groups for quinoline, are negative such that the contribution from these groups served to simply negate the regressed contribution of the adsorption capacity. We believe that the success of this regression was simply an artifact of the regression process and not reflective of any physicochemical process. Nevertheless, in the case of the negative coefficient of lactone for both quinoline and indole, it may not be only due to the artifact of the regression process. Moreno-castilla and coworkers^[34] reported that the carboxylic acid groups can transform to yield the lactone groups. This transformation reaction can be accelerated by the concentration of the carboxylic acid group, which would evidently decrease the adsorption capacity due to the reduction of the high-capacity carboxylic acid groups along with the increasing of the low-capacity lactone group. However, this possibility will be further confirmed in future work.

In addition, Fig. 5 shows the plots of the observed adsorption capacity for nitrogen compounds against the model-calculated adsorption capacity using this linear regression model relating the surface oxygen-containing functional groups to adsorption. The results showed that the experimental data were well predicted by this regression over a wide range of adsorption capacity, including one of the oxidized OAC10 sample, which showed very high adsorption capacity owing to its much higher concentration of oxygen-containing groups than those of commercial AC samples.

Thus, the present study verifies that the chemical properties of the ACs were the dominant factor for their ADN performance and that the ADN performance of the carbon-based adsorbents can be improved significantly by enhancement of the special oxygen-containing functional groups on the surface. Further studies with other treated samples, such as oxidation- and heat-treated AC samples, will be used to confirm the significance of the effect of the carboxylic acid groups on the adsorption of different nitrogen compounds and to investigate the applicability of these findings to other nitrogen compounds.

4 Conclusions

ADN performance of twelve AC samples was evaluated in a batch system using two solutions containing quinoline and indole in decane. The surface chemical properties, including the type and concentration of the oxygen-containing functional groups on the AC surface, were characterized by TPD-MS analysis based on the CO- and CO₂-evolution profiles. The adsorption was found to obey the Langmuir adsorption isotherm. The adsorption parameters (the maximum capacity and the adsorption constant) were estimated. The correlation between the adsorption performance of the AC samples and their chemical properties was investigated by a multiple linear-regression analysis, which showed that the types and the amounts of the oxygen-containing functional groups play a decisive role in the ADN using AC adsorbents. The acidic groups, especially the carboxylic acid functional groups, appear to be highly responsible for the adsorption of both basic and neutral nitrogen compounds. The present study implies that the ADN performance of carbon-based adsorbents can be improved significantly by enhancement of the special oxygen-containing functional groups on the surface.

Acknowledgments

The China Scholarship Council is gratefully acknowledged for supporting LI Na at Pennsylvania State University. This work was partially supported by the US Department of Energy through CPCPC Grant No: DE-FC26-03NT41874, Subcontract No: 3551-TPSU-DOE-1874. The authors thank Dr. WANG Xiao-xing and Dr. ZHU Jian for their assistance with

the TPD characterization.

References

- [1] Turaga UT, Ma X, Song C. Influence of nitrogen compounds on deep hydrodesulfurization of 4,6-dimethyldibenzothiophene over Al_2O_3 - and MCM-41-supported Co-Mo sulfide catalysts[J]. *Catalysis Today*, 2003, 86(1-4): 265-275.
- [2] Gutberlet L C, Bertolacini R J. Inhibition of hydrodesulfurization by nitrogen compounds[J]. *Industrial & Engineering Chemistry Product Research and Development*, 1983, 22(2): 246-250.
- [3] Choi K-H, Korai Y, Mochida I, et al. Impact of removal extent of nitrogen species in gas oil on its HDS performance: an efficient approach to its ultra deep desulfurization[J]. *Applied Catalysis B: Environmental*, 2004, 50(1): 9-16.
- [4] Sano Y, Choi K-H, Korai Y, et al. Effects of nitrogen and refractory sulfur species removal on the deep HDS of gas oil [J]. *Applied Catalysis B: Environmental*, 2004, 53(3): 169-174.
- [5] Yang H, Chen J, Fairbridge C, et al. Inhibition of nitrogen compounds on the hydrodesulfurization of substituted dibenzothiophenes in light cycle oil [J]. *Fuel Processing Technology*, 2004, 85(12): 1415-1429.
- [6] Furimsky E, Massoth F E. Deactivation of hydroprocessing catalysts[J]. *Catalysis Today*, 1999, 52(4): 381-495.
- [7] van Looij F, van der Laan P, Stork W H J, et al. Key parameters in deep hydrodesulfurization of diesel fuel[J]. *Applied Catalysis A: General*, 1998, 170(1): 1-12.
- [8] Almarri M, Ma X, Song C. Selective adsorption for removal of nitrogen compounds from liquid hydrocarbon streams over carbon- and alumina-based adsorbents[J]. *Industrial & Engineering Chemistry Research*, 2008, 48(2): 951-960.
- [9] Eijsbouts S, De Beer V H J, Prins R. Hydrodenitrogenation of quinoline over carbon-supported transition metal sulfides [J]. *Journal of Catalysis*, 1991, 127(2): 619-630.
- [10] Furimsky E, Massoth F E. Hydrodenitrogenation of Petroleum [J]. *Catalysis Reviews: Science and Engineering*, 2005, 47(3): 297-489.
- [11] Sano Y, Choi K-H, Korai Y, et al. Selection and further activation of activated carbons for Removal of Nitrogen Species in Gas Oil as a Pretreatment for Its Deep hydrodesulfurization[J]. *Energy & Fuels*, 2004, 18(3): 644-651.
- [12] Sano Y, Choi K-H, Korai Y, et al. Adsorptive removal of sulfur and nitrogen species from a straight run gas oil over activated carbons for its deep hydrodesulfurization[J]. *Applied Catalysis B: Environmental*, 2004, 49(4): 219-225.
- [13] Song C, Ma X. New design approaches to ultra-clean diesel fuels by deep desulfurization and deep dearomatization[J]. *Applied Catalysis B: Environmental*, 2003, 41(1-2): 207-238.
- [14] Wandas R, Chrapek T. Hydrotreating of middle distillates from destructive petroleum processing over high-activity catalysts to reduce nitrogen and improve the quality[J]. *Fuel Processing Technology*, 2004, 85(11): 1333-1343.
- [15] Egorova M, Prins R. Competitive hydrodesulfurization of 4,6-dimethyldibenzothiophene, hydrodenitrogenation of 2-methylpyridine, and hydrogenation of naphthalene over sulfided Ni-Mo/ γ - Al_2O_3 [J]. *Journal of Catalysis*, 2004, 224(2): 278-287.
- [16] Prins R, Egorova M, Rothlisberger A, et al. Mechanisms of hydrodesulfurization and hydrodenitrogenation [J]. *Catalysis Today*, 2006, 111(1-2): 84-93.
- [17] Song C. An overview of new approaches to deep desulfurization for ultra-clean gasoline, diesel fuel and jet fuel [J]. *Catalysis Today*, 2003, 86(1-4): 211-63.
- [18] Babich I V, Moulijn J A. Science and technology of novel processes for deep desulfurization of oil refinery streams; a review [small star, filled] [J]. *Fuel*, 2003, 82(6): 607-631.
- [19] Kim J H, Ma X, Zhou A, et al. Ultra-deep desulfurization and denitrogenation of diesel fuel by selective adsorption over three different adsorbents: A study on adsorptive selectivity and mechanism[J]. *Catalysis Today*, 2006, 111(1-2): 74-83.
- [20] Ellis J, Korth J. Removal of nitrogen compounds from hydro-treated shale oil by adsorption on zeolite [J]. *Fuel*, 1994, 73(10): 1569-1573.
- [21] Hernández-Maldonado A J, Yang R T. Denitrogenation of transportation fuels by zeolites at ambient temperature and pressure[J]. *Angewandte Chemie*, 2004, 116(8): 1022-1024.
- [22] Almarri M, Ma X, Song C. Role of Surface oxygen-containing functional groups in liquid-phase adsorption of nitrogen compounds on carbon-based adsorbents[J]. *Energy & Fuels*, 2009, 23(8): 3940-3947.
- [23] Boehm H P. Some aspects of the surface chemistry of carbon blacks and other carbons[J]. *Carbon*, 1994, 32(5): 759-769.
- [24] Yang Y. Determination of nitrogen compounds in catalytic diesel oil using gas chromatography [J]. *Chinese Journal of Chromatography*, 2008, 26(4): 478-483.
- [25] Zeuthen P, Knudsen K G, Whitehurst D D. Organic nitrogen compounds in gas oil blends, their hydrotreated products and the importance to hydrotreatment [J]. *Catalysis Today*, 2001, 65(2-4): 307-314.
- [26] Li N, Ma X, Zha Q, et al. Analysis and comparison of nitrogen compounds in different liquid hydrocarbon streams derived from petroleum and coal[J]. *Energy & Fuels*, 2010, 24(10): 5539-5547.
- [27] Figueiredo J L, Pereira M F R. The role of surface chemistry in catalysis with carbons[J]. *Catalysis Today*, 2010, 150(1-2): 2-7.
- [28] Figueiredo J L, Pereira M F R, Freitas M M A, et al. Characterization of active sites on carbon catalysts [J]. *Industrial & Engineering Chemistry Research*, 2006, 46(12): 4110-4115.
- [29] Zhou J H, Sui Z J, Zhu J, et al. Characterization of surface oxygen complexes on carbon nanofibers by TPD, XPS and FT-IR [J]. *Carbon*, 2007, 45(4): 785-796.
- [30] Figueiredo J L, Pereira M F R, Freitas M M A, et al. Modification of the surface chemistry of activated carbons [J]. *Carbon*, 1999, 37(9): 1379-1389.
- [31] Kohl S, Drochner A, Vogel H. Quantification of oxygen surface groups on carbon materials via diffuse reflectance FT-IR spectroscopy and temperature programmed desorption [J]. *Catalysis Today*, 2010, 150(1-2): 67-70.
- [32] Salame I I, Bandoz T J. Surface chemistry of activated carbons: combining the results of temperature-programmed desorption, boehm, and potentiometric titrations [J]. *Journal of Colloid and Interface Science*, 2001, 240(1): 252-258.
- [33] Boehm H P. Surface oxides on carbon and their analysis: a critical assessment [J]. *Carbon*, 2002, 40(2): 145-149.
- [34] Moreno-Castilla C, Carrasco-Marín F, Mueden A. The creation

of acid carbon surfaces by treatment with $(\text{NH}_4)_2\text{S}_2\text{O}_8$ [J].

Carbon, 1997, 35(10-11): 1619-1626.

活性炭表面含氧基团与其液相吸附脱氮性能的关系

李 娜^{1,2}, Masoud Almarri², 马筱良², 查庆芳¹

(1. 中国石油大学(华东) 化学化工学院, 山东 东营 257061;

2. 美国宾州州立大学 EMS 能源研究所, 209 Academic Project Building, University Park, PA 16802, USA)

摘 要: 选用 12 种物化学性质不同的活性炭, 利用 TPD 对活性炭表面含氧基团的种类和浓度进行考察, 使用质谱仪定量分析其含氧基团在不同温度下分解产生的 CO_2 和 CO , 并通过曲线分峰测定含氧基团的种类和浓度。同时研究了这些活性炭分别对萘烷中的喹啉和吡啶的吸附行为。研究发现: 活性炭的吸附符合 Langmuir 吸附热力学。根据吸附过程中的最大吸附量和吸附常数测定结果, 使用多元线性回归方法, 对活性炭表面含氧基团种类和浓度与吸附量间的关系进行了关联, 建立了含氧基团与吸附量间的定量关系。研究表明: 活性炭物理性质对其在萘烷吸附脱氮中没有明显影响, 而含氧官能团, 特别是含羧基的环氧官能团对其脱氮性能起关键性的作用。

关键词: 活性炭; 表面含氧基团; 吸附脱氮; 多元线性回归

通讯作者: 查庆芳, 教授. E-mail: chaqingf50@hotmail.com

作者简介: 李 娜(1982-), 女, 山东东营人, 博士研究生, 主要从事油品吸附脱氮相关研究. E-mail: leenaa82@hotmail.com

《新型炭材料》2010 年 SCI 影响因子 0.888

2010 年度 JCR (SCI 的《期刊引证报告》) 于 6 月 28 日发布, 《新型炭材料》(NEW CARBON MATER) 2010 年的影响因子为 0.888, 5 年影响因子为 0.833, 在全球入选 SCI 的 4 种碳学科期刊中排名第 3 位(总被引频次排名第 2)。2010 年 JCR 中碳学科期刊相关数据如下表所示。

Ranking is based on carbons journal and sort selections

Rank	Abbreviated Journal Title (linked to journal information)	ISSN	JCR Data						Eigenfactor™ Metrics	
			Total Cites	Impact Factor	5-Year Impact Factor	Immediacy Index	Articles	Cited Half-life	Eigenfactor™ Score	Article Influence™ Score
1	CARBON	0008-6223	23839	4.893	5.724	1.023	559	6.3	0.05867	1.602
2	CHEM PHYS CARBON	0069-3138	334	4.750	5.250			>10.0	0.00011	1.400
3	NEW CARBON MATER	1007-8827	413	0.888	0.833	0.087	80	4.5	0.00097	0.157
4	FULLER NANOTUB CAR N	1536-383X	301	0.631	0.610	0.164	73	4.4	0.00123	0.178

《新型炭材料》编辑部